Long non-coding RNA SREBF2-AS1 promotes cell progression by increasing SREBF2 expression in Hepatocellular carcinoma

Lili Qu
Nanjing Medical University Second Affiliated Hospital
Xiaoxiao Cai
nantong maternal and child health hospital affiliated to nantong university
Lailing Gong
Nanjing Medical University ANanjing Medical University Second Affiliated Hospital
Peng Shen
the affiliated huaian No.1 People's hospital nanjing medical university
Yefei Zhu
Nanjing Medical University Second Affiliated Hospital
Mei Jiao
Nanjing Medical University Second Affiliated Hospital
chuan su (qulili@njmu.edu.cn)
Nanjing Medical University https://orcid.org/0000-0001-8108-9745

Research

Keywords: Hepatocellular carcinoma, lncRNAs, SREBF2-AS1, sterol regulatory element-binding protein 2 (SREBF2)

Posted Date: December 22nd, 2020

DOI: https://doi.org/10.21203/rs.3.rs-131876/v1

Abstract

Background

Hepatocellular carcinoma (HCC) is one of the most common malignancies worldwide. Long non-coding RNAs (lncRNAs) are emerging as one of important regulators that may be involved in the progression of cancers in humans.

Methods

Comprehensive analysis of the lncRNA expression profile of HCC was performed by using TCGA and Gene Expression Omnibus (GEO) database to screen the target lncRNA(s). LncRNA of SREBF2-AS1 was selected and its expression level in a cohort of 15 pairs of HCC tissues was verified by quantitative real-time PCR (qRT-PCR). Loss-of-function and gain-of-function assays were carried out to investigate the role of SREBF2-AS1 in HCC progression in vitro. Tumor formation assay was performed to verity the role of SREBF2-AS1 in HCC progression in vivo.

Results

Database analysis showed that the expression of SREBF2-AS1 was upregulated in HCC, which was correlated with neoplasm grade and over survival time. The expression of SREBF2-AS1 was verified in a cohort of 15 pairs of HCC tissues. SREBF2-AS1 knockdown mitigated HCC cell growth and promoted apoptosis in vitro and in vivo. Whereas, SREBF2-AS1 overexpression promoted tumor cell growth. Furthermore, our investigation demonstrated that the oncogenic activity of SREBF2-AS1 is partially attributable to the regulation of sterol regulatory element-binding protein 2 (SREBF2) expression.

Conclusions

Our study highlights the regulatory role of SREBF2-AS1 in promoting HCC progression, suggesting that SREBF2-AS1 might be a potent therapeutic target by regulating the expression of SREBF2 for patients with HCC.

Background

Up to 2018, liver cancer ranks the sixth most common cancer and is the fourth most fatal cancer in the world, in which hepatocellular carcinoma (HCC) accounts for 75%-85% [1]. The progression of HCC mainly related to chronic infection with hepatitis B, hepatitis C virus, smoking, drinking, aflatoxin contaminated food, and obesity [2]. However, the molecular pathogenesis of HCC remains unclear. Advances in molecular and cell biology, detailed characterizations of genomes, epigenomes, proteomes, and metabolomes in HCC have provided new insights into hepatic carcinogenesis [3].

Accumulating evidence based on high-throughput sequencing technology suggests that noncoding RNAs (ncRNAs) constitute more than 90% of the RNAs [4], and participate in various physiological and pathological process [5]. Recently, as a novel member of ncRNA, long noncoding RNAs (lncRNAs) with more than 200 nucleotides in length have attracted attention [6, 7]. LncRNAs are implicated in influencing gene expression at transcriptional, post-transcriptional, and epigenetic levels [8]. Recently, although some lncRNAs have been reported to be implicated in the occurrence and progression of HCC [9], the expression pattern and regulatory mechanisms need further study [10].

Development of the high-throughput RNA sequencing techniques and bioinformatics methods emerge as promising and helpful tools for screening of genetic alterations in carcinogenesis and discovering new biomarkers for cancers [11]. In particular, integrating multiple microarray datasets could provide convincing results [12]. In this study, we aimed to identify novel candidate lncRNAs that contribute to the progression of HCC. We compared the lncRNAs profiles of HCC and adjacent non-tumor tissues based on TCGA RNA sequencing data and two Gene Expression Omnibus (GEO) RNA sequencing and microarray datasets (GSE GSE55191 and GSE67260).

Our results showed that SREBF2-AS1 was upregulated in HCC and the expression level of SREBF2-AS1 was associated with poor prognosis, perhaps due to the regulation of HCC cells proliferation and apoptosis through regulating sterol regulatory element-binding protein 2 (SREBF2).

Results

Screening of DElncRNAs in HCC

To find novel lncRNAs involved in HCC tumorigenesis, 50 paired HCC and normal tissues in TCGA and two microarray gene profiling data (GSE55191 and GSE67260) were utilized. Results revealed that 387 DElncRNAs were dysregulated in the TCGA dataset (294 up-regulated and 93 down-regulated), 232 DElncRNAs in the GSE55191 dataset (139 up-regulated and 93 down-regulated), and 125 DElncRNAs in the GSE67260 dataset (65 up-regulated and 60 down-regulated) (Figs.1a-1f). Further intersection analysis revealed that SREBF2-AS1, PRKAR2A-AS1 and TM4SF1-AS1 were consistently up-regulated in these three datasets (Fig.1g). Thus, we pay more attention to these three lncRNAs most likely owing to their oncogenic ability.

Prognostic assessment of DElncRNAs profiles

The univariate and multivariate Cox analysis between clinical features and HCC were performed to confirm the prognostic significance of the clinical characteristics. As shown in table 1, clinical Neoplasm type, Pathological M stage and SREBF2-AS1 were significantly correlated with OS, which indicated that SREBF2-AS1 may be an important risk factor influencing the progression of HCC.

Expression of SREBF2-AS1 in HCC and Clinical Characteristic

We observed similarly significant upregulation of SREBF2-AS1 in HCC specimens and cell lines, consistent with the results shown in TCGA (Figs. 2a-2c). To further explore the relationship between SREBF2-AS1 and clinical Characteristic data of HCC patients, clinicopathological characteristics were divided into different groups. Due to the lack of survival time, 340 cases were included for univariate and multivariate Cox analysis, and since the missing of clinical information, 307 cases were included for clinical characteristic analysis. As shown in table 2 and Fig. 2e, SREBF2-AS1 was correlated with histologic grade. These results revealed that SREBF2-AS1 can be used for effective risk stratification in HCC. By Kaplan-Meier and Cox's proportional hazards regression model analysis we found that SREBF2-AS1 level was significantly correlated with poor OS of HCC patients (Fig. 2d).

SREBF2-AS1 regulated HCC cellular phenotypes *in vitro*

Since SREBF2-AS1 was located in the cytoplasm of HCC cells (Fig. 3a), we performed loss-of-function study in Huh7 and HepG2 using three discrete chemically synthesized siRNAs to manipulate the SREBF2-AS1 level in HCC cells. After 24 h of transfection, si-SREBF2-AS1-3 showed the best knockdown effect, which reduced the level of SREBF2-AS1 by 70% (Fig. 3b). We renamed si-SREBF2-AS1-3 as si-SREBF2-AS1 in the following experiments. CCK8 assay demonstrated that knockdown of SREBF2-AS1 inhibited the proliferation rate of Huh7 and HepG2 (Fig. 3c). Meanwhile, colony formation assay showed that downregulation of SREBF2-AS1 significantly attenuated the colony-forming ability of HCC cells (Fig. 3d), as well as an increased percentage of Huh7 and HepG2 cells in G0/G1 phase (Fig. 3e). Furthermore, knockdown of SREBF2-AS1 increased the apoptosis of HCC cells in si-SREBF2-AS1 group (Fig. 3f). Simultaneously, we transfected cell with pcDNA3.1- SREBF2-AS1 vector, and found that of SREBF2-AS1 promoted cell growth (Figs. 3g and 3h). These results indicated that SREBF2-AS1 could promote HCC.

Knockdown of SREBF2-AS1 inhibited HCC tumorigenesis *in vivo*

Compared with the NC group, tumor volume and weight in si-SREBF2-AS1 group were significantly lower (Figs. 4a-4d). By HE staining we observed typical characteristics of tumor cells, and the Ki-67 staining showed low proliferative activity of the HCC cells in si-SREBF2-AS1 group (Fig. 4e). Moreover, the expression level of SREBF2-AS1 in the si-SREBF2-AS1group were lower (Fig. 4f). Collectively, these data indicated that SREBF2-AS1 knockdown suppressed HCC growth *in vivo*.

Higher expression of SREBF2 in HCC

Based on the bioinformatics analysis, we found that 265 bp of SREBF2-AS1 overlapped with the first exon 1 of SREBF2 (Fig. 5a), which may lay the structural foundation of the regulatory relationship between the two molecules. We observed similarly significant upregulation of SREBF2 in HCC specimens and cell lines as well as in TCGA, which was similar with the expression pattern of SREBF2-AS1 (Figs. 5b-5f).

SREBF2-AS1 regulated SREBF2 expression in HCC

To identify the association between SREBF2-AS1 and SREBF2, we first detected SREBF2-AS1 and SREBF2 mRNA expression levels in SREBF2-AS1 and si-SREBF2-AS1 treated cells by qRT-PCR and western blotting. SREBF2 mRNA and protein levels in Huh7 and HepG2 cells transfected with SREBF2-AS1 were higher than those in NC (Figs. 6a and 6b), while SREBF2-AS1 knockdown significantly reduced SREBF2 mRNA and protein levels (Figs. 6c and 6d). Similar results were observed in xenograft model (Figs. 6e-6f). Importantly, the CCK8 assay and flow cytometry assays showed that the abilities of cell growth and apoptosis by SREBF2-AS1 over expression were partially counteracted by SREBF2 knockdown (Figs. 6g, 6i), as well as a decreased percentage of Huh7 and HepG2 cells in G0/G1 phase (Fig. 6h).

Discussion

HCC carcinogenesis is a multi-step process involving various genetic and environmental factors, while molecular mechanisms are still poorly understood. Recent studies have focused on lncRNAs in HCC pathogenesis [13, 14]. Bioinformatic data mining of gene expression data provides a helpful tool for revealing lncRNAs alterations in tumorigenesis and progression by epigenetic regulation, transcription and posttranscription regulation [15]. Since individual data investigation often shows a bias due to insufficient numbers of specimens, integrating multiple individual data has been considered as a better approach of enhancing the reliability of results [16].

In present study, we observed that SREBF2-AS1 was upregulated and correlated with the prognosis of HCC and promoted cell progression by increasing SREBF2 expression. For lncRNA, its biological function mainly determined by the subcellular localization. Here, we found that SREBF2-AS1 was mainly located in the cytoplasmic base on FISH analysis, which implicated that SREBF2-AS1 mainly participated in post-transcriptional regulation. SREBF2-AS1 is classified as antisense (AS) lncRNAs that are reverse complements of endogenous sense counterparts [17], account for 50–70% of ncRNAs. Antisense lncRNAs appear to function in a locus-specific effects on their neighboring protein-coding genes including suppression, activation, or homeostatic adjustment [18]. For example, PCNA-AS1 binds PCNA mRNA and forms a lncRNA: mRNA duplex to promote tumor growth by enhancing PCNA mRNA stability in HCC [19]. While AChE-AS exerts an anti-apoptotic effect via epigenetic modification of AChE promoter to repress AChE expression in HCC cells [20]. These divergent evidences suggest a potential mechanism of LncRNA: antisense lncRNAs hybridized with cognate mRNA to form a duplex for gene transcriptional regulation by promoter activation to post-transcriptional regulation by controlling mRNA stability and translatability. However, the mechanisms by which the vast majority antisense lncRNAs function, exerting any activity, remain largely unknown. There are two regulation types between an antisense lncRNA and its cognate sense mRNA: discordant or concordant. Our data suggested that SREBF2-AS1 and SREBF2 are expressed in a concordant manner. Mechanisms of concordant regulation have been explored in previous investigations, however, why the antisense lncRNAs can exert biologically effects on its sense partner without being expressed in equimolar amounts remains incompletely understood [21]. Moreover, why the RNA duplex has no impact on mRNA translation need further explored.

SREBF2 is a vital regulator of genes associated with cholesterol biosynthesis, the key component of cell membranes of proliferating cells [22]. Previous study demonstrated that SREBF2 as a regulator of HMGCR, was increased in esophageal squamous cell carcinoma and promoted the migration and invasive abilities [23]. Also, aberrant SREBF2 expression has been associated with prostatic cancer progression probably due to the regulation of cholesterol and other lipids [24]. So, SREBF2 metabolic pathway impairment is proposed as potential anti-tumor approach [25]. In addition, Chen demonstrated that the reactivation of the MAPK pathway determined an up-regulation of SREBF proteins promoting metastatic prostatic cancer [24]. In this study, we demonstrated that the expression of SREBF2 was upregulated in HCC, in accordance with Jiang's report [26]. Furthermore, we found that the inhibition of SREBF2 in HCC cells induced an anti-tumor activity.

Conclusions

In summary, our study revealed an oncogenic role for SREBF2-AS1 upregulation in HCC. Additionally, we reported for the first time that the activity of SREBF2-AS1 is attributable to its regulation of SREBF2, which may open avenues for utilizing lncRNAs to insight into the molecular mechanism of HCC.

Methods

Datasets

Clinical information and RNA sequencing data of HCC and paired normal tissues were downloaded from TCGA data up to February 7, 2019. HCC RNA sequencing and microarray datasets GSE55191 and GSE67260 downloaded from GEO datasets was analyzed using Affymetrix Human Genome U133 Plus 2.0 Array. The differently expressed lncRNAs (DElncRNAs) between HCC tumor and adjacent normal tissues were screened using edgeR package of the R platform, with adjusted $P< 0.05$ and the thresholds of |log2FC| >2.0.

Survival analysis and Clinical significance of DElncRNAs

The association of each lncRNA expression level and overall survival (OS) was calculated by univariate Cox model. Then, the contribution of lncRNA as independent prognosis factors of OS was evaluated via multivariate Cox analysis. Kaplan-Meier curves of DElncRNA was plotted using the "survival" package in R software with $P< 0.05$.

The association of LncRNA with clinicopathological characteristics of HCC patients**,** including age (over or under 60 years), gender (male or female), clinical stage (I, II or III, IV), histologic grade (G1,G2,G3 or G4), Pathologic(T,N,M), and risk factors (alcohol consumption, hepatitis B, hepatitis C, no history of primary risk factors and non-alcoholic fatty liver disease) were analyzed with $P<0.05$.

Tissue collection

Fifteen paired HCC tumors and adjacent normal tissues were collected from HCC patients without any local or systemic anticancer treatment before surgical resection at the Second Affiliated Hospital of Nanjing Medical University. The specimens were collected during surgery, and immediately kept in RNA Later stabilization solution (Invitrogen, USA) and froze. Ethics approval was obtained from the Ethics Committee of the Second Affiliated Hospital of Nanjing Medical University and written informed consent was obtained from all participants.

Cell culture and transfection

Human normal liver cell line L02 and HCC cell lines HepG2, Hep3B, and Huh7 used in this study were stored in our laboratory. They were cultured in Dulbecco's modified Eagle's medium (DMEM, GIBCO, USA), supplemented with 10% heat-inactivated fetal bovine serum (GIBCO, USA), 100 U/mL penicillin, and 100 μg/mL streptomycin in a humidified incubator with 5% CO_2 atmosphere at 37°C. The siRNAs sequences were chemically synthesized by Gene Pharma Company (China) and listed as follows: SREBF2-AS1, si-1: 5'-CCAUCAUACAUGCCUGCAATT-3'; si-2:5'-CGUCCGGUCAUCAUCUUAAT-3'; si-3:5'-GCAGCUGGUCGUGUUGUAA TT-3'. si-SREBF2: 5'-GCUGGUAAAUGGUGUGAUUTT-3'. Negative control (NC): 5'-UUCUCCGAACGUGUCACGUT T-3'. For tumor assay in nude mouse model, siRNAs were modified by 2OMe + 5Chol (Ribobio, China). Full-length SREBF2-AS1 cDNA was synthesized and subcloned into pcDNA3.1 vector (Genebay, China). Cells in the logarithmic growth phase at 70% confluence were transfected with siRNAs or vectors by lipofectamine 3000 reagent (Invitrogen, USA).

Fluorescence in situ immunohybridization (FISH)

The probe of SREBF2-AS1 was designed and synthesized by Invitrogen (Shanghai, China), and its sequences were 5'-ACGCACCGCTTCGCTCGCCCATTG G-3'. Cells were fixed in 4% formaldehyde, washed, and treated with pepsin K for 3 min. Next the cells were air-dried and incubated with FISH probe diluted in hybridization buffer. After the hybridization, the cells were washed, dehydrated, and visualized under a fluorescence microscope (DMI4000B, Leica, German).

RNA isolation and detection of lncRNA and mRNA

The total RNA was isolated from cell lines or tissue samples using TRIzol® reagent (Invitrogen, USA) and reversely transcribed to cDNA using HiScript® II Q RT SuperMix kit (Vazyme, China). Then, qRT-PCR analyses were performed using the SYBR Green PCR Master Mix (ThermoFisher, USA). The primers were as follows: GAPDH (forward: 5'-TGT GGGCATCAATGGATTTGG-3', reverse: 5'-ACACCATG TATTCCGGGTCAAT-3'), SREBF2-AS1 (forward: 5'-GTCATCCAATCCCGCTTC T-3', reverse:5'-GTTCCGA GGTGCCAGAGATT-3'), SREBF2 (forward: 5'-CAGAC ATCATCTGTCGGTGG T-3' and reverse: 5'-CGCAA TGGCAGAAGGAACTC-3'). The relative gene expression was analyzed by $2^{\triangle\triangle ct}$ method in triplicate

Western blot analysis

Proteins were extracted from cells or tissue samples using RIPA buffer containing Phenyle methane sulfonyl fluoride (Beyotime, China). Proteins were separated by SDS-PAGE and transferred onto PVDF membranes, which were then blocked with 5% non-fat milk in Tris-buffered saline with 0.05% Tween-20 (TBST) and incubated overnight with following primary antibodies: rabbit polyclonal antibody SREBF2(Abcam, USA) and mouse monoclonal antibody GAPDH (Abmart, China). The membranes were washed with TBST and then incubated with horseradish peroxidase conjugated secondary antibodies: goat anti-rabbit IgG (Biosharp, China) or goat anti-mouse IgG (Abmart). Finally, the immunoreactive protein bands on the membrane were visualized using an ECL Kit (Beyotime, China).

Cell proliferation assay

Cells proliferation was evaluated using Cell Counting Kit-8 assays (CCK8) (Dojindo Laboratories, Japan). Huh7 and HepG2 cells transfected by siRNAs after 24h were seeded into the 96-well plates at a density of 5,000 cells/well and then incubated for 0 h, 24 h, 48 h and 72 h. Subsequently, 10 μl CCK8 solution was added to each well and incubated for 2 h at 37˚C. The optical density (OD) of 450 nm was measured by a microplate reader.

Colony formation assay

Huh7 and HepG2 cells were transfected by siRNAs and after 24 h were seeded into 6-well plates with 500 cells per well. After culture for two weeks, most of the colonies contained at least 50 cells, the colonies were fixed in methanol and stained with 0.1% crystal violet.

Flow-cytometric analysis for apoptosis and cell cycle

For apoptosis assay, Huh7 and HepG2 cells were harvested after transfection for 24h. Firstly, 5×10^5 cells were suspended in binding buffer and stained by Annexin V-FITC and Propidium Iodide (PI) (BD Biosciences, USA). Secondly, cells were vortexed and then incubated for 15-20 min after mixing, and immediately subjected to flow cytometry within an hour. For cell cycle assay, cells were collected and fixed using 70% ethanol at -20 ˚C for 18 h, and stained with 400 ul of propidium iodide (PI) for 30 min. The results were analyzed with FlowJo software (FlowJo LLC, USA).

Xenograft model

Nude mice (male, five-weeks old) were subcutaneously injected with 1×10^7 HepG2 cells randomly and divided into two groups (n=5). When tumors grew to 50 mm^3, siRNAs modified by 2OMe + 5Chol were injected into tumors in si-SREBF2-AS1 group every two days, while NC group were injected with control siRNAs. Tumor diameter was measured every two days by digital calipers. After three weeks, the mice were sacrificed and the tumor size and weight were measured. The protocol and procedures employed were ethically reviewed and approved by Animal Ethical and Welfare Committee of NJMU.

Immunohistochemistry

The tissues were fixed in 4% paraformaldehyde, embedded in paraffin, and cut into sections (4 μm thin). After antigen retrieval, the sections were blocked with bovine serum albumin, and incubated with primary antibody at 4°C overnight. Next, the sections were incubated with horseradish peroxidase-conjugated secondary antibody at room temperature for 1 h, and staining signal was detected with Tissue Staining HRP-DAB Kit (DAKO).

Statistical analysis

Data were analyzed using GraphPad Prism 7 (GraphPad, USA). The comparison of two groups was performed using Student's t-test, and analysis between multiple groups was conducted by one-way analysis of variance (ANOVA) with the Bonferroni correction. *P* value< 0.05 indicated significant difference.

Abbreviations

ANOVA: one-way analysis of variance; AS:antisense; CCK8:Cell Counting Kit-8 assays; DElncRNAs:differently expressed lncRNAs; GEO:Gene Expression Omnibus; HCC:hepatocellular carcinoma; lncRNAs:long non-coding RNAs; NC:negative control; ncRNAs:noncoding RNAs; OD:optical density; OS:overall survival; PI:propidium iodide; qRT-PCR:quantitative real-time PCR; SREBF2:sterol regulatory element-binding protein 2.

Declarations

Acknowledgements

Not applicable.

Authers' contributions:

Chuan Su conceived the idea and designed the experiment; Lili Qu and Xiaoxiao Cai conducted experiments and data analysis; Lailing Gong, Peng Shen and Mei Jiao collected the specimens; Lili Qu and Xiaoxiao Cai wrote the manuscript; Yefei Zhu revised the manuscript.

Founding

This study was supported by The Second Affiliated Hospital of Nanjing Medical University Medical Development and Support Fund, Jiangsu Provincial "333 project" Fund for High-level Talent Cultivation (No. BRA2018086) and The Science and Technology Development Foundation of Nanjing Medical University of China (No.2016NJMUZD03).

Availability of data and materials

The data that support the findings of this study are available from the corresponding author upon reasonable request.

Ethics approval and consent to participate

All animal experiments were approved by Animal Ethical and Welfare Committee of NJMU. All procedures performed in studies involving human participants were in accordance with the ethical standards of the Ethics Committee of the Second Affiliated Hospital of Nanjing Medical University.

Consent for publication

Written informed consent was obtained from the patients and participants for publication of their individual details in this manuscript. The consent form is held by the authors and is available for review by the Editor-in-Chief.

Competing interests

The authors declare no potential conflict of interest.

Author details

[1]State Key Lab of Reproductive Medicine, Jiangsu Key Laboratory of Pathogen Biology, Department of Pathogen Biology and Immunology, Center for Global Health, Nanjing Medical University, Nanjing, China

[2]Laboratory Medicine Center, The Second Affiliated Hospital, Nanjing Medical University, Nanjing, China

[3]Laboratory Medicine Center, Nantong Maternal and Child Health Hospital Affiliated to Nantong University, Nantong, China

[4]The affiliated Huaian No.1 People's Hospital Nanjing Medical University, Huaian, China

References

1. Bray F, et al. Global cancer statistics 2018: GLOBOCAN estimates of incidence and mortality worldwide for 36 cancers in 185 countries. CA Cancer J Clin 2018;68:394-424.

2. Mak LY, et al. Global Epidemiology, Prevention, and Management of Hepatocellular Carcinoma. Am Soc Clin Oncol Educ Book 2018;38:262-79.

3. Huang W, et al. Advances in genomic hepatocellular carcinoma research. Gigascience 2018;7:giy135.

4. Slack FJ, et al. The Role of Non-coding RNAs in Oncology. Cell 2019;179:1033-55.

5. Cech TR, et al. The noncoding RNA revolution-trashing old rules to forge new ones. Cell 2014;157:77-94.

6. Bartel DP. Metazoan MicroRNAs. Cell 2018;173:20-51.

7. Evans JR, et al. The bright side of dark matter: lncRNAs in cancer. J Clin Invest 2016;126:2775-82.

8. Kopp F, et al. Functional Classification and Experimental Dissection of Long Noncoding RNAs. Cell 2018;172:393-407.

9. DiStefano JK. Long noncoding RNAs in the initiation, progression, and metastasis of hepatocellular carcinoma. Noncoding RNA Res 2017;2:129-36.

10. Ma Z, et al. The expanding roles of long non-coding RNAs in the regulation of cancer stem cells. Int J Biochem Cell Biol 2019;108:17-20.

11. Blum A, et al. SnapShot: TCGA-Analyzed Tumors. Cell 2018;173:530.

12. Li Y, et al. Transcriptomic and functional network features of lung squamous cell carcinoma through integrative analysis of GEO and TCGA data. Sci Rep 2018;8:15834.

13. Huang Z, et al. The role of long noncoding RNAs in hepatocellular carcinoma. Mol Cancer 2020;19:77.

14. Pea A, et al. Biology and clinical application of regulatory RNAs in hepatocellular carcinoma. Hepatology 2020. doi: 10.1002/hep.31225.

15. Zhang H, et al. Identification of the molecular mechanisms underlying dilated cardiomyopathy via bioinformatic analysis of gene expression profiles. Exp Ther Med 2017;13:273-9.

16. Cui H, et al. A comprehensive genome-wide analysis of long noncoding RNA expression profile in hepatocellular carcinoma. Cancer Med 2017;6:2932-41.

17. Katayama S, et al. Antisense transcription in the mammalian transcriptome. Science 2005;309:1564-66.

18. Villegas VE, et al. Neighboring gene regulation by antisense long non-coding RNAs. Int J Mol Sci 2015;16:3251-66.

19. Yuan SX, et al. Antisense long non-coding RNA PCNA-AS1 promotes tumor growth by regulating proliferating cell nuclear antigen in hepatocellular carcinoma. Cancer Lett 2014;349:87-94.

20. Xi Q, et al. A natural antisense transcript regulates acetylcholinesterase gene expression via epigenetic modification in Hepatocellular Carcinoma. Int J Biochem Cell Biol 2014;55:242-51.

21. Balbin OA, et al. The landscape of antisense gene expression in human cancers. Genome Res 2015;25:1068-79.

22. Shimano H. Sterol regulatory element-binding proteins (SREBPs): transcriptional regulators of lipid synthetic genes. Prog Lipid Res 2001;40:439-52.

23. Zhong C, et al. SREBP2 is upregulated in esophageal squamous cell carcinoma and cooperates with cMyc to regulate HMGCR expression. Mol Med Rep 2019;20:3003-10.

24. Chen M, et al. An aberrant SREBP-dependent lipogenic program promotes metastatic prostate cancer. Nat Genet 2018;50:206-18.

25. Li X, et al, Huang WC. Fatostatin displays high antitumor activity in prostate cancer by blocking SREBP-regulated metabolic pathways and androgen receptor signaling. Mol Cancer Ther 2014;13:855-66.

26. Jiang Y, et al. Proteomics identifies new therapeutic targets of early-stage hepatocellular carcinoma. Nature 2019;567:257-61.

Tables

Table 1. **Univariate and multivariate analysis of clinicopathological characteristics and lncRNAs with overall survival in TCGA cohort.**

Univariate analysis			Multivariate analysis	
	HR (95% CI)	P value	HR (95% CI)	P value
TCGA LIHC set (n= 340)				
Age (> 60 year vs ≤60 year)	0.641 (0.401-1.025)	0.06	0.686 (0.423-1.111)	0.12
Gender (Male vs Female)	1.567 (0.989-2.483)	0.121	1.433 (0.887-2.315)	0.144
Pathological stage (T1+T2 vs T3 +T4)	1.568 (0.957-2.568)	0.074	1.668 (1.546-2.164)	0.099
Neoplasm_type (G1 + G2 vs G3 + G4)	**1.265 (0.8-2.002)**	**0.021**	**1.537 (0.934-2.53)**	**0.033**
Pathologic_T (T1+T2 vs T3 +T4)	1.638 (1.271-2.684)	0.05	1.728 (1.562-2.251)	0.095
Pathologic_N (N1 vs N2)	1.398 (0.839-2.33)	0.049	0.939 (0.489-1.806)	0.065
Pathologic_M (M1 vs M2)	**2.261 (1.398-3.658)**	**< 0.001**	**2.549 (1.363-4.767)**	**0.003**
SREBF2-AS1 (> Median vs ≤ median)	**0.891 (0.566-1.402)**	**0.032**	**0.959 (0.605-1.52)**	**0.048**
PRKAR2A-AS1 (> Median vs ≤ median)	0.951 (0.602-1.502)	0.083	1.078 (0.652-1.782)	0.076
TM4SF1-AS1 (> Median vs ≤ median)	0.9 (0.57-1.42)	0.045	0.956 (0.592-1.546)	0.053

Table 2. The relationship between SREBF2-AS1 and clinical features with hepatocellular carcinoma patients in TCGA.

Clinical features	TCGA			
	Case(n)	Low(n)	High(n)	P-value
Sample	307	153	154	
Age				0.6089
> 60 year	160	77	83	
≤ 60 year	147	76	71	
Gender				0.1324
Male	208	97	111	
Female	99	56	43	
Clinical stage				0.8714
	162	79	83	
	76	41	35	
	65	31	34	
	4	2	2	
Neoplasm type				0.0071
G1	37	10	27	
G2	150	72	78	
G3	108	64	44	
G4	12	7	5	
Pathologic T				0.2464
1	164	80	84	
2	77	41	36	
3	59	31	28	
4	7	1	6	
Pathologic N				0.7715
0	222	109	113	
1	85	44	41	
Pathologic M				0.9892
0	231	115	116	

1	76	38	38	
Risk factors				0.3677
Alcohol consumption	49	22	27	
Hepatitis B	101	55	46	
Hepatitis C	41	16	25	
No History of Primary	107	54	53	
Risk Factors				
Non-Alcoholic	9	6	3	
Fatty Liver Disease				

Figures

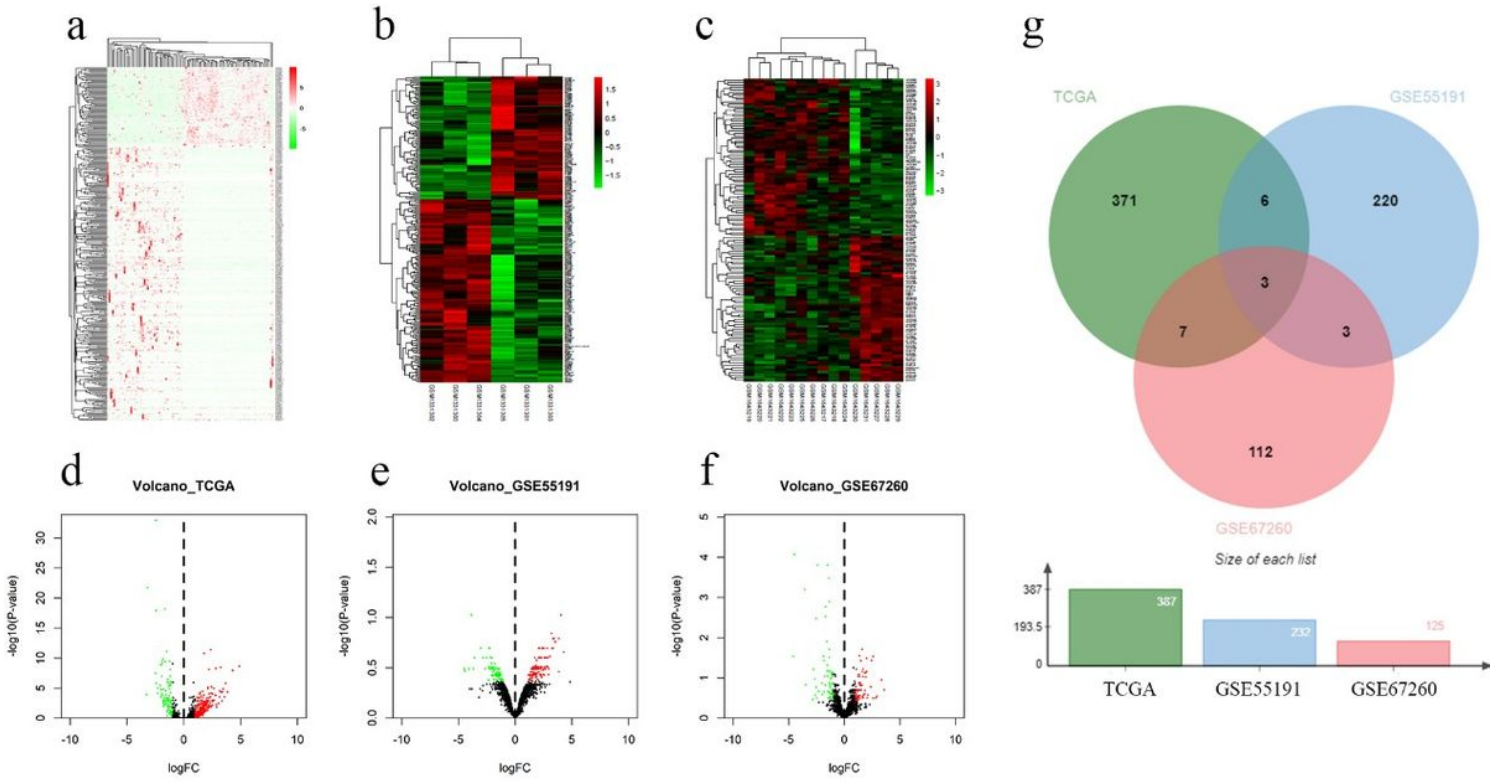

Figure 1

Differential expressed analysis of RNAs from HCC patients compared with normal samples. a Heatmap of the DElncRNAs in HCC and normal tissue samples was analyzed using the TCGA datasets. b, c Heatmap of the DElncRNAs in HCC was analyzed using the GSE55191, GSE67260 datasets. DElncRNAs were hierarchically clustered by R software a-c respectively. The left longitudinal axis indicated the cluster analysis of DERNAs, and the right axis denoted the results of DElncRNAs a-c, respectively. The upper

horizontal axis denoted the cluster analysis of each sample, and the down axis below the map corresponded to the results. Each RNA analysis was plotted into the volcano map, and red color represented the upregulated DElncRNAs d-f with log FC ≥ 2 while green represented the downregulated DElncRNAs with log2 FC < 2. g Venn diagram of DElncRNAs in TCGA, GSE55191 and GSE67260. FC, fold change; DE, differential expressed.

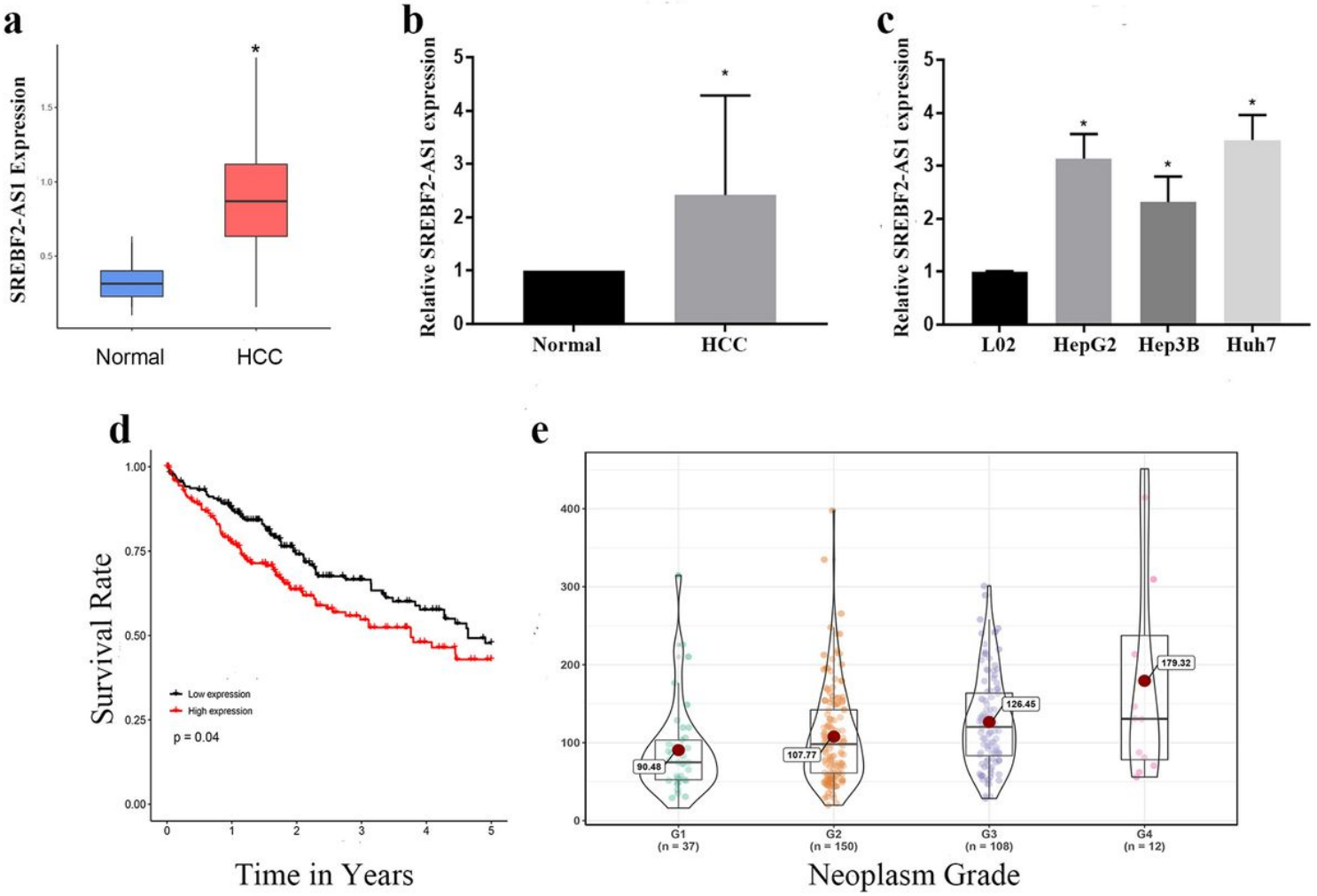

Figure 2

Higher SREBF2-AS1 expression levels in HCC and its clinical significance. a The SREBF2-AS1 expression levels in HCC tissues compared with normal tissues in TCGA. b The SREBF2-AS1 expression level in 15 HCC tissues and corresponding adjacent non-tumor tissues was quantified by qRT-PCR analysis and normalized to GAPDH expression. c The SREBF2-AS1 expression level in one normal liver cell line and three HCC cell lines were quantified by qRT-PCR analysis and normalized to GAPDH expression. d Kaplan-Meier survival plots demonstrated that higher SREBF2-AS1 abundance correlated with a poor OS, using TCGA data from 340 HCC patients. e The relationship between SREBF2-AS1 expression and clinicopathological parameters neoplasm grade was shown. *P<0.05.

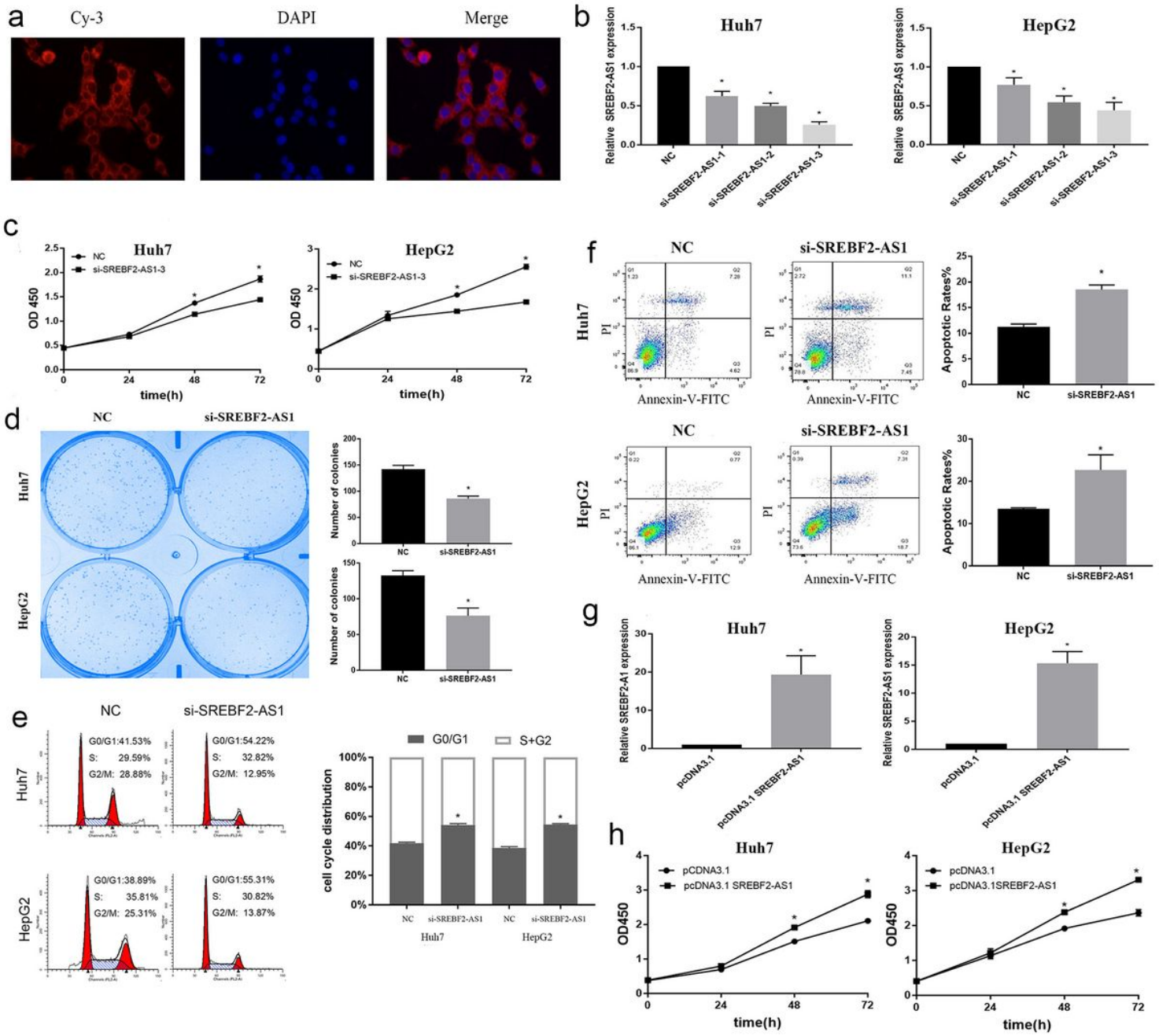

Figure 3

The effects of SREBF2-AS1 on HCC cell viability in vitro. a FISH analysis showed that SREBF2-AS1 is located in the cytoplasm. b The SREBF2-AS1 expression level in Huh7 and HepG2 transfect with three discrete chemically synthesized siRNAs. c CCK8 assays were used to measure the growth curve of si-SREBF2-AS1-3 transfected Huh7 and HepG2 cells. Values indicate the mean ± SD from three independent experiments. d Colony-forming assays were conducted to determine the proliferation of si-SREBF2-AS1-3 transfected Huh7 and HepG2 cells. e Flow cytometry detection of cell cycle of Huh7 and HepG2 cells. f The apoptosis of Huh7 and HepG2 were analyzed by flow cytometry. g The SREBF2-AS1 expression level in Huh7 and HepG2 transfected with pcDNA3.1 SREBF2-AS1and empty vector pcDNA3.1. h CCK8 assays

were used to measure the growth curve of pcDNA3.1 SREBF2-AS1 transfected Huh7 and HepG2 cells. *P<0.05.

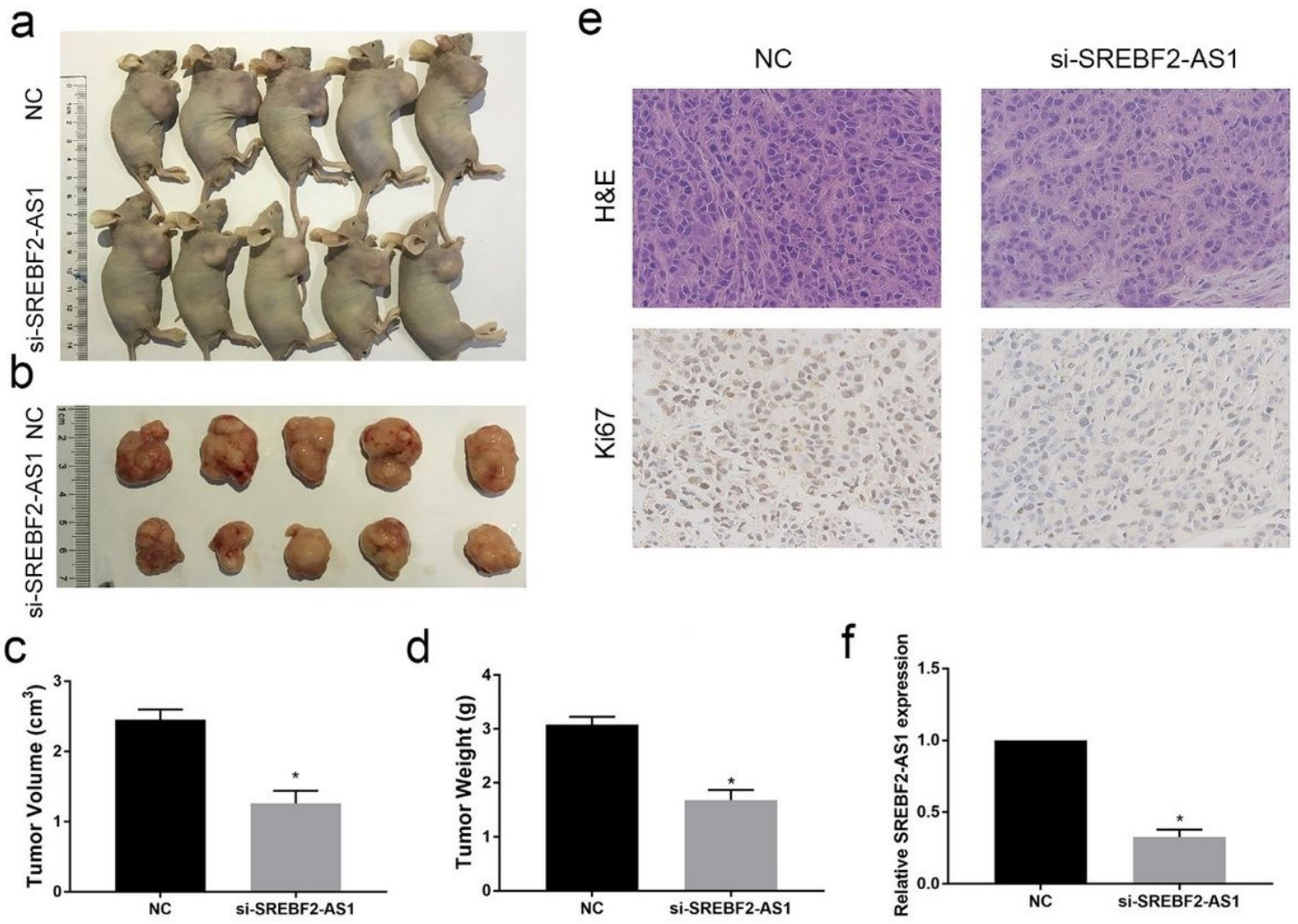

Figure 4

The effects on tumor growth after SREBF2-AS1 downregulation in vivo. a -c The tumor volume was calculated every 3 days when tumors grew to 50 mm3 measured 7 days after the injection of HepG2 cells and siRNAs modified by 2OMe + 5Chol and were injected every 3 days. d Tumor weight when the tumors were harvested. e Representative images of HE staining and Ki-67 immunohistochemistry of the tumor. f qRT-PCR analysis of SREBF2-AS1 expression level in tumor tissues formed from NC and si-SREBF2-AS1injected HepG2 cells. *P<0.05.

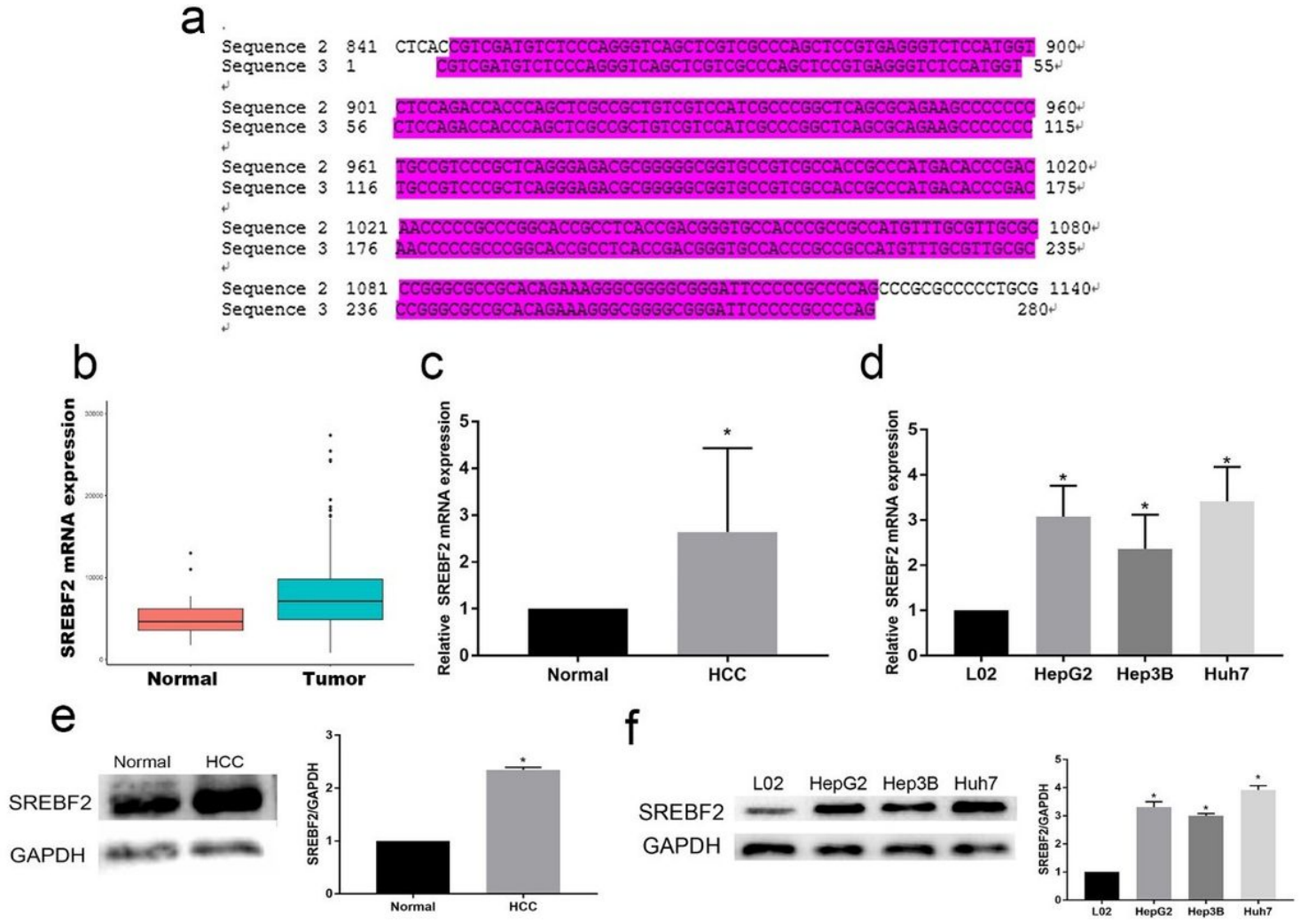

Figure 5

Higher SREBF2 expression levels in HCC. a The target gene of SREBF2-AS1 was predicted through bioinformatics. Complementary binding was identified that 265 bp of SREBF2-AS1overlapped with the first exon 1 of SREBF2 sequences. b The SREBF2 mRNA expression levels in HCC tissues compared with normal tissues in TCGA. c, d The SREBF2 mRNA expression level in 15 HCC tissues and corresponding adjacent non-tumor tissues, and one normal liver cell line and three HCC cell lines were quantified by qRT-PCR analysis and normalized to GAPDH expression. e, f The western blot analysis was conducted to detect the expression levels of SREBF2 protein in 15 HCC tissues and corresponding adjacent non-tumor tissues, and one normal liver cell line and three HCC cell lines. *P<0.05.

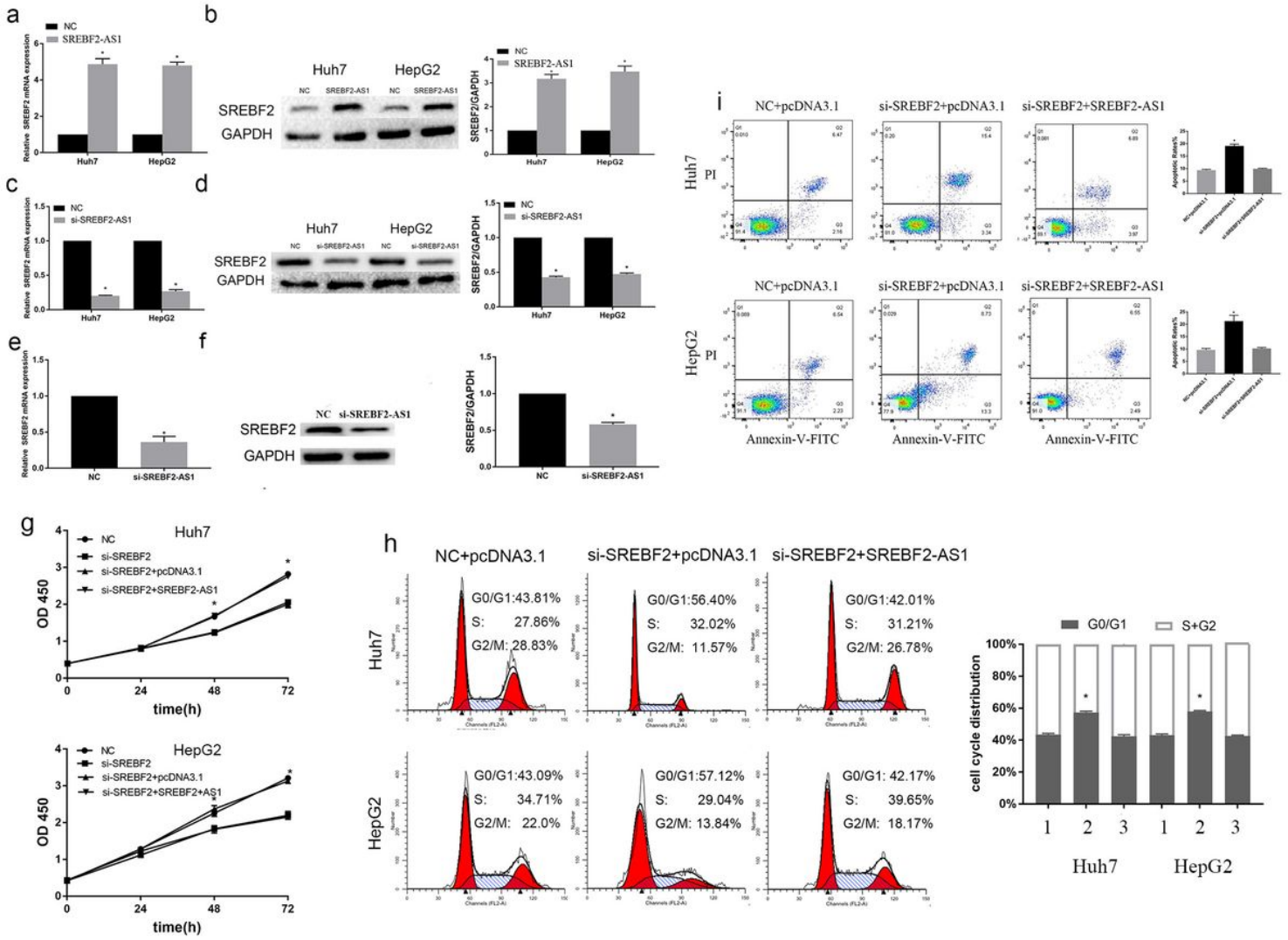

Figure 6

SREBF2-AS1 regulates SREBF2 expression in HCC. a, b The expression level of SREBF2 mRNA and protein in Huh7 and HepG2 cells transfected with SREBF2-AS1 and NC. c, d The expression level of SREBF2 mRNA and protein in Huh7 and HepG2 cells transfected with si-SREBF2-AS1 and si-NC. e, f The expression level of SREBF2 mRNA and protein in HepG2 cells injected with si-SREBF2-AS1 and si-NC in vivo. g CCK8 assays were used to measure the growth curve of SREBF2-AS1+NC and SREBF2-AS1+si-SREBF2 transfected Huh7 and HepG2. h Flow cytometry detection of cell cycle of Huh7 and HepG2 cells transfected with NC+pcDNA3.1, si-SREBF2+pcDNA3.1 and si-SREBF2+SREBF2-AS1. (1、NC+pcDNA3.1; 2、si-SREBF2 + pcDNA3.1; 3、si-SREBF2+ SREBF2-AS1) i The apoptosis of Huh7 and HepG2 were analyzed by flow cytometry. *P<0.05.